# Influence of Dispersant Addition on the Rise of Oil Droplets Contributions to Modelling

Sophie Van Ganse[1], Stéphane Le Floch[1]
Rudy Mauge[2], Aprin Laurent[3]

[1] Cedre, Centre de Documentation, de Recherche et d'Expérimentations sur les pollutions accidentelles des eaux, Brest Cedex 2, France
[2] Alyotech Technologies, Rennes, France
[3] LGEI, Ecole des Mines d'Alès, Ales Cedex, France
stephane.le.floch@cedre.fr

**Abstract**

For many years, Oil & Gas industry stakeholders have clearly expressed their need for tools to predict and model oil and gas leaks. The accident involving the Deepwater Horizon platform in the Gulf of Mexico in April 2010 confirmed the importance of fully understanding these underwater phenomena and their consequences at the sea surface. While the modelling of the rise of oil droplets in the water column is widely documented, in particular through mathematical equations in which the notion of slip velocity appears, little information is available on the effect of dispersants on oil droplet rise. Yet dispersants, given their surfactant capacity, will necessarily alter the shape of oil droplets and, by extension, their behaviour in the water column, in particular in terms of buoyancy.

The aim of this paper is to discuss the physical changes undergone by an oil droplet when surface active molecules are positioned at its interface with seawater. For the population of oil droplets, it was shown that the addition of dispersant decreases the average droplet volume and therefore increases the number of droplets observed in the water column. Thus, the water-oil contact surface area is increased, which leads to an increase in exchanges between these two phases, in particular in terms of the dissolution of the lightest hydrocarbon molecules. In terms of physical appearance, oil droplets lose their spherical shape and take on an elliptical shape to which filaments of varying sizes are attached. This change in shape implies a variation in the oil droplet's slip velocity within the seawater column as well as the definition of a more complex trajectory. These two changes tend to decrease the buoyancy of oil droplets in the water column which results in the formation of a plume, which is carried by marine currents, rather than a surface oil slick.

In conclusion, this project aims to characterise the fate of oil droplets with added dispersant in the water column following release from the bottom, in order to define mathematical equations to model this fate.

## 1    Introduction

Since the second half of the twentieth century, the increase of world demography and economic developments have led to an increase in energy requirements. Among all energies, oil remains the most coveted and consumed in the world. With four billion tons in 2010, oil represents almost 33.6% of the total energetic expense. This oil demand involves risks of pollution during extraction and transport. During the last decades, many maritime accidents have occurred, resulting in major releases of oil into the environment (Torrey Canyon, 1967; Amoco Cadiz, 1978; Exxon Valdez, 1989).

During the response to these accidents, dispersants were widely used to promote the transfer of oil slicks from the surface to the water column, and therefore reduce the amount of

oil washing up on the shore. Furthermore, the addition of dispersant promotes the dilution of the oil and, by stabilising the oil droplets in the water column, increases the degradation activity of micro-organisms able to use carbon from the oil to develop (Campo et al., 2013; Prince et al., 2013). Based on this argument, for the first time in the history of oil spill response, dispersants were added to oil escaping from an offshore well during the Deepwater Horizon (DWH) spill in 2010. During the DWH spill, 4000 $m^3$ of dispersant where spread on the water surface, and more than 3 000 $m^3$ where injected underwater (leak at 1 500m depth). This response strategy immediately reduced the quantities of oil arriving at the surface but raised a certain number of questions concerning the fate of the dispersed oil, in particular in terms of understanding this fate. Modelling software commonly used to predict these fates provided results which were removed from reality, doubtlessly due to the presence of dispersant at the oil-water interface. It therefore appeared necessary to work on the mathematical equations which describe the fate of an oil droplet within a water column in order to take into account the influence of this chemical dispersion (Yapa et al.,2004).

## 2      Physical Model

In plumes, there is a slip velocity between rising fluid particles and the surrounding liquid within the plume area. Slip velocity $w_s$ in a droplet plume is the velocity difference between rising droplets and the surrounding liquid.

The most commonly used law to calculate this slip velocity is based on the Stokes law. For the smallest single isolated droplets, which are approximately perfect spheres due to the dominant effect of surface tension on their shape, Stokes' solution provides a reasonably accurate description such as (Equation 1):

Equation 1:
$$w_s = \frac{g d_e^2 (\rho_l - \rho_g)}{18 \mu_l}$$

Where $d_e^2$ is the equivalent particle diameter and $\mu_l$ the dynamic viscosity of liquid. This law holds by assuming the particle to be small, spherical, rigid and for a Reynolds number smaller than one ( $Re = \frac{\rho_l d_e w_s}{\mu_l} \leq 1$), i.e. for a laminar terminal velocity. For larger and more turbulent particles, we may use (Equation 2):

Equation 2:
$$w_s = \sqrt{\frac{4}{3} \frac{g \, \Delta\rho \, d_p}{\rho_w \, C_D}}$$

Where $\Delta\rho$ is the difference in density with the fluid environment ( $\rho_w$ ), $d_p$ is the diameter of the fluid particle, $\upsilon_w$ is the water kinematic viscosity and $C_D$ is the drag coefficient. These velocities are representative for small and large fluid particles where the viscosity of ambient fluid is a crucial factor for the smallest whereas the largest are governed by the equilibrium between the drag and buoyancy forces.

Clift et al. (1978) have shown that the shape of fluid particles could be approximated as a sphere for the small size range (smaller than 1 mm), an ellipsoid in the intermediate size range (1 mm to 15 mm), and a spherical-cap in the larger size range. For the spherical bubbles, the terminal velocity is influenced by the viscosity of the ambient fluid, for the

ellipsoidal bubbles the interfacial tension is the key factor, while neither the viscosity of the ambient fluid nor interfacial tension influence the spherical-cap bubbles.

Clift et al. (1978) offer several correlations for the different regimes of bubble shapes.

- The regime of spherical shape is given by (Equation 3):

Equation 3:
$$w_s = \frac{\mu R_e}{\rho d}$$

The criterion in this regime is d $<10^{-3}$m.

- The regime of ellipsoidal shape is given by (Equation 4):

Equation 4:
$$w_s = \frac{\mu_l}{\rho_l d_e} M^{-0.149} ( J - 0.857 )$$

Where

$J = 0.94 H^{0.757}$ for $2 < H \le 59.3$

$J = 3.42 H^{0.441}$ for $H > 59.3$

$H$ is defined as $H = \frac{4}{3} E_0 M^{-0.149} \left( \frac{\mu}{\mu_w} \right)^{-0.14}$ with $\mu_w$ the dynamic viscosity of water;

$E_0$ the Eötvös number defined as follows: $E_0 = \frac{g( \rho_l - \rho_g )d_e^2}{\sigma}$ with $\sigma$ the interfacial tension;

$M$ the Morton number defined as follows: $M = \frac{g \mu^4 \Delta \rho}{\rho^2 \sigma^3}$

The criteria in this regime are M$<10^{-3}$ and Eo$<40$.

- The regime of spherical-cap is given by (Equation 5):

Equation 5:
$$w_s = 0.711 \sqrt{\frac{g d_e^2 ( \rho_l - \rho_g )}{\rho_l}}$$

The following figure illustrates the terminal velocity according to the effective diameter for a single isolated oil droplet.

LeFloch, S., S. Van Ganse, R. Mauge, and A. Laurent, Influence of Dispersant Addition on the Rise of Oil Droplets Contribution to Modelling, Proceedings of the Thirty-sixth AMOP Technical Seminar on Environmental Contamination and Response, Environment Canada, Ottawa, ON, pp. 315-325, 2013.

The figure shows a plot with title $\rho_{oil} = 700 kg/m^3$ - $\sigma_G = 32.00 mN/m$, with Terminal Velocity (m/s) on the y-axis and Diameter (m) on the x-axis.
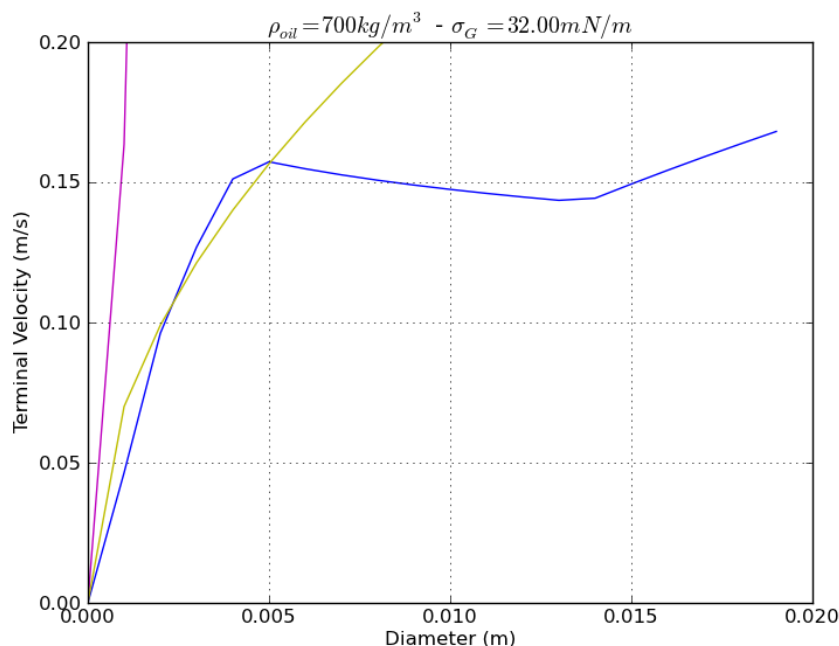
**Figure 1: Slip velocity for an oil droplet with a laminar formulation (magenta curve), turbulent formulation (yellow curve) and Clift's formulation (blue curve).**

The standart's law, based on the stoke's law, curves in magenta (laminar formulation) and yellow (turbulent formulation) are often used in numerical models. The blue curve is given by Clift's formulation presented in this paper. The comparison of the three curves shows that using Clift's formulation the predicted rise velocity is highly different. As described in the previous paragraphs, Clift's formulation takes into account the interfacial tension between the particles and water, ignored in the two other formulations.

## 3 Experiments in the *Cedre* Experimental Column (CEC)
To aim of this experimental investigation is to compare the behaviour of oil and dispersed oil in the water column. It is designed to observe the shape of the droplets, their rise trail, and if possible their dissolution rate during their ascension to the surface.

### 3.1 The *Cedre* Experimental Column
The *Cedre* Experimental Column (CEC) is equipped with an injection system, on which it is possible to set nozzles of different diameters, and two high speed video recording systems. The CEC is a five meter high hexagonal column with a diameter of 1 m and a total capacity of 4.50 m$^3$. The experimental design, presented in Figure 1, is described by Le Floch et al. (2009). The first camera is located 15 cm above the injection nozzle (4 m depth), at a pressure of 141325 Pa, and the second, 15 cm below the surface (0.15 m depth), at a pressure of 102825 Pa. The distance between the 2 recording systems is 3.65 m. During the experiments the temperature was 784.15 K.

LeFloch, S., S. Van Ganse, R. Mauge, and A. Laurent, Influence of Dispersant Addition on the Rise of Oil Droplets Contribution to Modelling, Proceedings of the Thirty-sixth AMOP Technical Seminar on Environmental Contamination and Response, Environment Canada, Ottawa, ON, pp. 315-325, 2013.
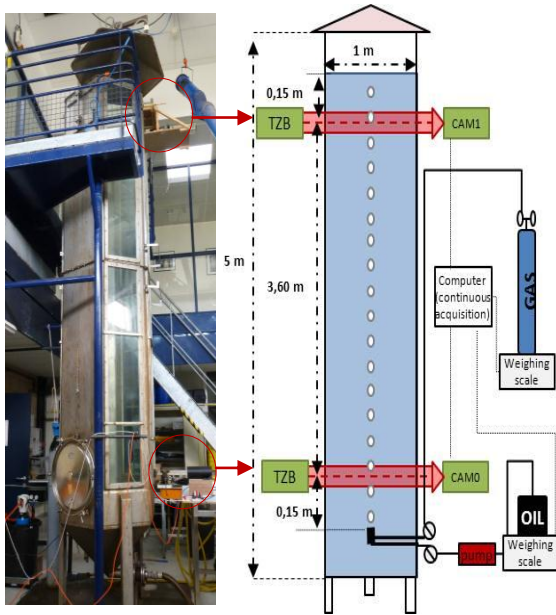
**Figure 2: Cedre Experimental Column designed with shadowgraphy equipment (2 laser and camera in a parallel plan) and bubble injection system of gas or/and oil from the bottom (4 m depth).**

### 3.2     Products and Experimental Conditions

A light Arabian crude oil was used in this research in order to study its behaviour differences in the water column. To characterise droplets, the viscosity of the oil needs to be low, otherwise the injected oil forms filaments instead of droplets. The Arabian oil was selected because of its low viscosity of 10.2 cSt at 15°C. The density of the oil was 0.844. The dispersed oil was a prepared mixture of Arabian oil and 5% volume of dispersant (Corexit 9500).

The injections, performed at 3.90 m depth, were achieved by a 50 cm long stainless steel injection tube combined with a nozzle. This injection was performed with an injection nozzle of 1.5 mm in diameter, at 1700 rpm, at a flow rate of 30 ml/min (at atmospheric pressure) helped by a pump. At this flow rate, droplets are close together and may interact; the outlet pressure is low in order to avoid jet dynamics.

### 3.3     High Speed Video Records by Shadowgraph Technique

The experiments performed in the CEC were conducted by a shadowgraph approach (Settles, 2001). As presented in Figure 1, at 2 different depths, a telecentric lights vicolux TZB95 provided continuous red light illumination on a Nikkor lens 105mm-SVS340 muge (CAM0 and CAM1), which recorded the event (Slangen et al., 2010). The cameras recorded 64 frame.s$^{-1}$ with a resolution of 640 x 840 pixels. The area of interest (center of the column), represented 3.42 x 2.57 cm, for CAM0 (bottom) and 2.46 x 1.85 cm for CAM1 (surface) corresponding respectively to a pixel resolution of 53.5 µm and 38.5 µm. Each sequence of image was processed to locate and track the gas bubble with the help of the NI-vision software. This tracking, based on the detection of differences of grey levels for each pixel on the image, isolated the bubble (dark) from the background (bright). The time separating 2 images, 15.6 ms, and the position of the centre of the bubble on the X and Y axes of the image, allowed the bubble velocity (m.s$^{-1}$) to be calculated. The waddel disk diameter is

LeFloch, S., S. Van Ganse, R. Mauge, and A. Laurent, Influence of Dispersant Addition on the Rise of Oil Droplets Contribution to Modelling, Proceedings of the Thirty-sixth AMOP Technical Seminar on Environmental Contamination and Response, Environment Canada, Ottawa, ON, pp. 315-325, 2013.

defined as the diameter of the disk with the same area as the particle[1] (Fuhrer et al., 2011). The Heywood circularity factor was calculated to describe the shape of the particle, the closer the shape of the particle is to a disk, the closer this factor is to 1. The calculation of this factor corresponds to the ratio of a particle perimeter to the perimeter of the circle with the same area[2].

## 4.     Results
### 4.1     Particle Shape without and with Dispersant

For the same injection conditions, the shape, and consequently the behaviour, of oil droplets and dispersed oil droplets were very different. Table 1 presents images of the droplets at 4 m depth and 0.15 m depth.

Pure oil provided spherical-shaped particles at both depths. The Heywood circularity factor (HCF) confirms the homogeneity of the oil droplets population, which were spherical for sizes ranging between 0 and 6.3 mm.

Oil with added dispersant provided filament-shaped, ellipsoidal and a few spherical-shaped particles. With dispersant (oil + 5%.vol. dispersant) the HCF confirms that the droplets had various types of shapes and are highly different at 4 m depth and 0.15 m depth. In this condition, the effect of dispersant is clearly observed: with addition of dispersant the oil droplets' shape changed during their ascension in the water column. The droplets were flatter and lost an important amount of matter, forming filaments and smaller droplets, due to physical erosion processes linked to the friction force and also solubilisation processes.

---

[1] $2\sqrt{\text{particle area}}/\sqrt{\Pi}$
[2] Particle perimeter/$(2\sqrt{\Pi}*\text{particle area})$

**Table 1: Shape of oil droplet and dispersed oil droplet at 4 m depth and 0.15 m depth.**

| | At 4 m depth | | At 0.15 m depth | |
|---|---|---|---|---|
| **OIL** |  | Spherical shape **Heywood circularity factor** mean: 1.05±0.05 minimum value: 0.83 maximum value:1.43 |  | Spherical shape **Heywood circularity factor** mean: 1.01±0.04 minimum value: 0.84 maximum value:1.34 |
| **OIL + DISPERSANT** |  | Spherical, ellipsoidal and filaments shaped **Heywood circularity factor** mean: 1.14±0.05 minimum value: 0.75 maximum value: 3.45 |  | Spherical, ellipsoidal and "jellyfish" shaped **Heywood circularity factor** mean: 1.11±0.26 minimum value: 0.76 maximum value: 2.513 |

## 4.2    Particle Distribution with and without Dispersant

The sizes of the droplets were compared in both conditions, with and without dispersant, at the two different depths. Concerning the oil without dispersant, three different particle populations were observed; one with an equivalent diameter between 0.2 and 0.8 mm, mainly represented at 4 m depth with a frequency of 60% of the droplets, the other between 3 and 3.7 mm (8% at 4 m depth and 17.5% at 0.15 m depth) and the last group mainly represented at 0.15 m, with a frequency of 60%, between 0.3 and 5.4 (Figure 2).
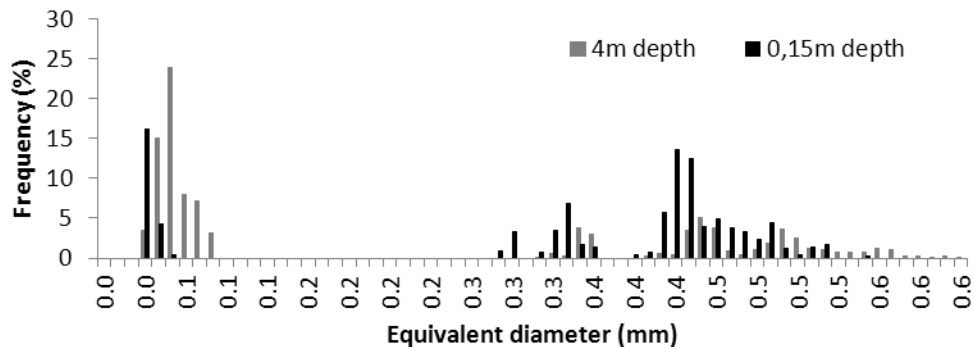


**Figure 3: Particle distribution at 4 m depth and 0.15 m depth for oil.**

In the case of dispersed oil, at 4 m depth the majority of the droplets were smaller than 1 mm (over 37% of the total) and larger droplets appeared between 1 mm and 6 mm. At 0.15 m more than 88% of the droplets ranged between 0 and 1 mm (Figure 3).
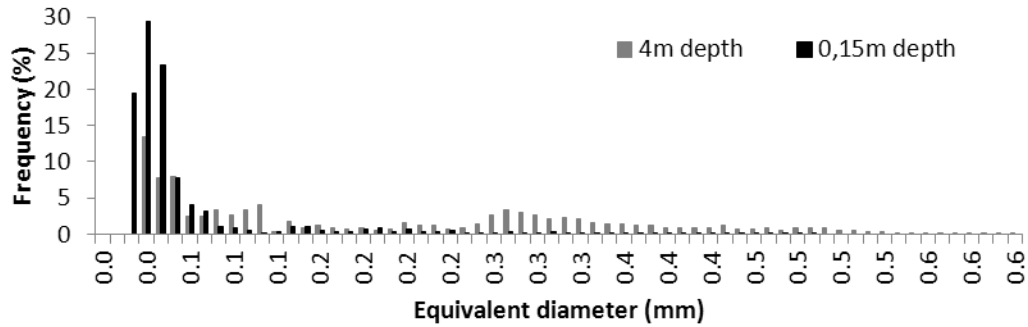
**Figure 4: Particle distribution at 4 m depth and 0.15 m depth for dispersed oil (5% of dispersant).**

These results clearly show that without dispersant, the oil droplets coalesced during their ascension in the water column (higher percentage of small particles at 4 m than at 0.15 m). When dispersant was added to oil, a higher percentage of small droplets (more than 88%) were obtained at 0.15 m than at 4 m depth which indicates that the larger droplets were divided during their rise to the surface.

### 4.3    Velocity of Oil Droplets in the Water Column with and without Dispersant

As explained in the theoretical part of this paper (part 2, physical model). The velocity of the droplet is influenced by the size of the particle, and the Clift formulation showed that this relationship is not linear (Clift, 1987; Li et al., 2000)

The experimental data, shown in Figure 5, concerning the rise velocity of oil particles without dispersant confirmed this approach. Indeed, the velocity obtained for the droplets at 4 m depth and 0.15 m did not present a linear relationship with the droplet size. The first group of data seems to follow a different equation to the second group of data. This difference can be explained by the different shape characterising these droplets. When the droplet are smaller than 1 mm their shape is spherical, whereas the larger droplets are more ellipsoidal shaped. Some intermediate points are missing on this graph to allow us to draw conclusions on the critical diameter at which the droplets change from spherical behaviour to ellipsoidal shape.
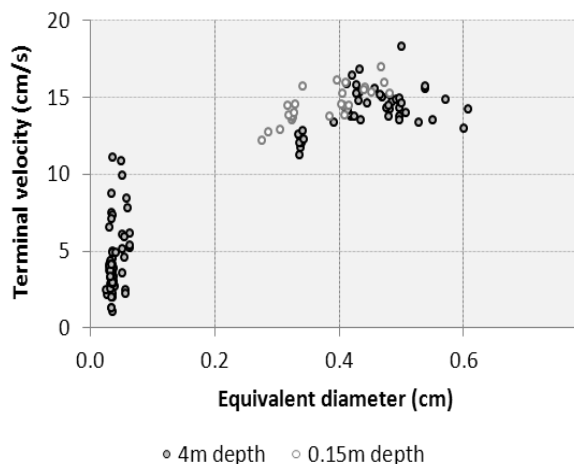


**Figure 5: Terminal velocity (cm/s) of oil droplets depending on the equivalent diameter (mm)**

LeFloch, S., S. Van Ganse, R. Mauge, and A. Laurent, Influence of Dispersant Addition on the Rise of Oil Droplets Contribution to Modelling, Proceedings of the Thirty-sixth AMOP Technical Seminar on Environmental Contamination and Response, Environment Canada, Ottawa, ON, pp. 315-325, 2013.

Concerning the oil droplets with dispersant, the experimental data are presented in Figure 6. These results clearly show the non-linear relationship between the equivalent diameters of the droplets with their terminal velocity. Also, for one equivalent diameter, we note a high standard deviation of velocity. This may be explained by the interactions between the droplets. The tendency of this standard deviation may be of interest in order to be linked with the interactions between the droplets in further experiments.

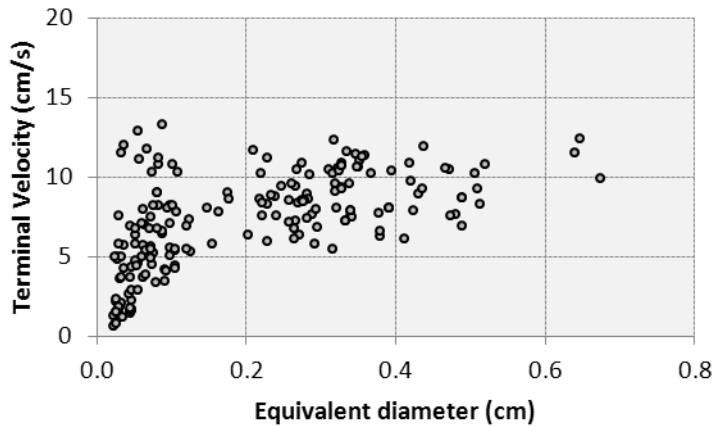Nevertheless, the terminal velocity limit seems to be lower when dispersant is added (<15 cm/s).



**Figure 6:** Terminal velocity (cm/s) of oil droplets depending of the equivalent diameter (mm)

## 4.4. Correlation between Experimental Data and Numerical Models

The comparison of the velocity of the oil droplets with and without dispersant is shown in Figures 7 and 8. The first consideration, which needs to be statistically strengthened with additional data, is that the addition of dispersant seems to decrease the rise velocity of the droplets of intermediate sizes, larger than 3 mm. For both conditions, for some particles smaller than 1 mm, the behaviour of the droplets seems to follow a laminar formulation (magenta curve), whereas some other particles seem to follow the turbulent formulation or the Clift's formulation. For the larger particles, above 3 mm, two different behaviours were observed. The oil droplets without dispersant (green) follow the Clift's curve plotted with an interfacial tension value of 32 mN/m (Fig. 7). However, the oil droplets with dispersant follow the Clift's curve plotted with an interfacial tension value of 0.86 mN/m  (Fig. 8). This result indicates that the addition of dispersant greatly decreases the interfacial tension of the oil droplets. And a decrease in this interfacial tension results in a decrease in the rise velocity of the oil droplets.
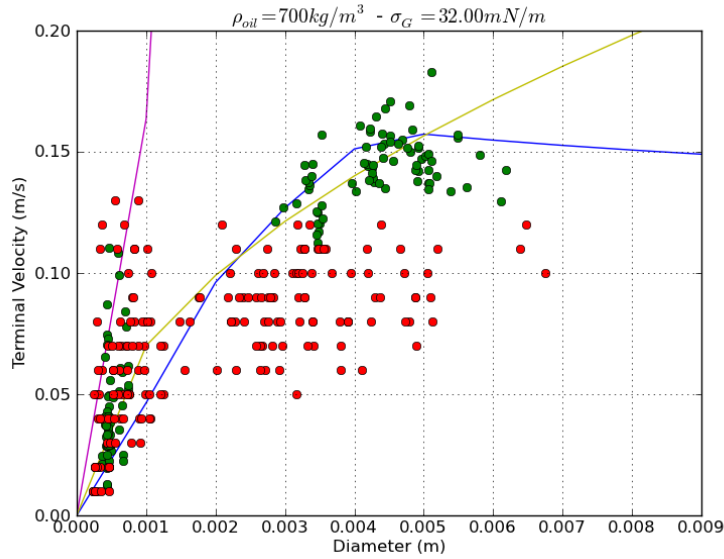
**Figure 7. Terminal velocity (m/s) of oil droplets with dispersant (red) and oil droplets without dispersant depth (green). Slip velocity for an oil droplet with a laminar formulation (magenta curve), turbulent formulation (yellow curve) and Clift's formulation for an interfacial tension of 32 mN/m (blue curve).**
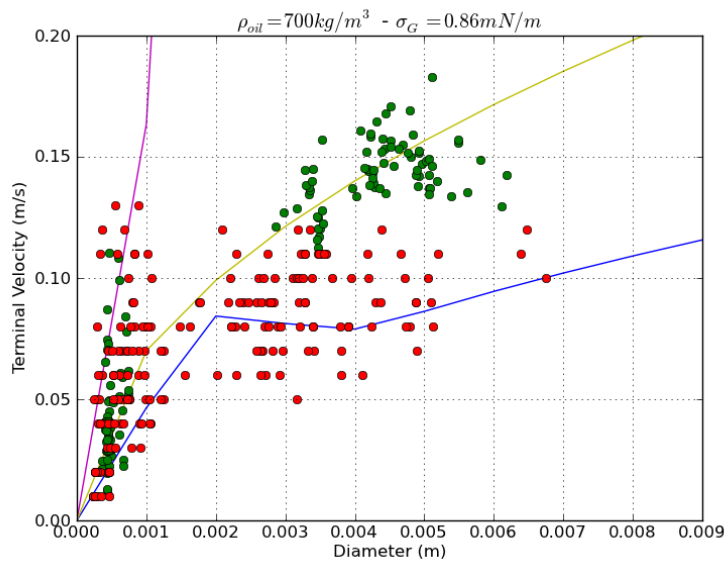


**Figure 8. Terminal velocity (m/s) of oil droplets with dispersant (red) and oil droplets without dispersant depth (green). Slip velocity for an oil droplet with a laminar formulation (magenta curve), turbulent formulation (yellow curve) and Clift's formulation for an interfacial tension of 0.86 mN/m (blue curve).**

## 5      Conclusion

In this paper, promising experimental results are presented regarding the behaviour differences between oil droplets and oil with added dispersant in the water column. On-going experimentation, using the same approach, will increase the number of samples and strengthen the confidence in these results from a statistical point of view.

However, as a preliminary conclusion, it can be said that dispersant addition reduces the size of oil droplets and changes their shape, and in doing so alters their rise velocity within

LeFloch, S., S. Van Ganse, R. Mauge, and A. Laurent, Influence of Dispersant Addition on the Rise of Oil Droplets Contribution to Modelling, Proceedings of the Thirty-sixth AMOP Technical Seminar on Environmental Contamination and Response, Environment Canada, Ottawa, ON, pp. 315-325, 2013.

the seawater column. While dispersant may reduce the surface tension of oil droplets, it also appears to prevent the coalescence of droplets and increases their dissolution.

These physico-chemical phenomena should be taken into account in software models designed to predict the fate of a subsea oil leak. Currently, Clift's equations appear to be the most suitable although questions remain over the interfacial tension values to be used. This work deserves to be supplemented by experiments designed to characterise the fate of oil droplets for various injection rates and also by varying the pressure within the water column.

## 6 References

Campo P., A.D. Venosa, and M.T. Suidan, "Biodegradability of Corexit 9500 and Dispersed South Louisiana Crude Oil at 5 and 25 degrees C", *Environmental Science & Technology,* 47:1960-1967, 2013.

Clift, R., J.R. Grace, and M.E. Weber, *Bubbles, Drops and Particles*, Academic Press, New York, 1978.

Fuhrer, M., P. Slangen, L. Aprin, G. Dusserre, and S. Le Floch, "A New Approach to Analyze Chemical Releases Behavior in Water Column: High Speed Imaging", *Proceedings of 2011 International Oil Spill Conference (IOSC),* Portland, Oregon, USA, 23-26 May, 21, 2011.

Le Floch, S., H Benbouzid, "Operational Device and Procedure to Test Initial Dissolution Rate of Chemicals after Ship Accidents: The Cedre Experimental Column, *The open Environmental Pollution and Toxicology Journal* 1:1-10, 2009.

Li, Z. and P.D. Yapa, "Buoyant Velocity of Spherical and Non-spherical Bubbles/Droplets", *Journal of Hydraulic Engineering*, Members ASCE, 126:852-854, 2000.

Reddy, C.M., J.S. Arey, J.S. Seewald, S.P. Sylva, K.L. Lemkau, R.K. Nelson, C.A. Carmicheal, C.P. Mclntyre, J. Fenwick, G.T. Ventura, B.A.S. Van Mooy, and Richard Camilli, "Composition and Fate of Gas and Oil Released to the Water Column during the *Deepwater Horizon* Oil Spill", *PNAS*, Vol. 109, No. 50, pp. 20229-20234, 2012.

Prince R.C., K.M. McFarlin, J.D. Butler, E.J. Febbo, F.C.Y. Wang, and T.J. Nedwed, "The primary biodegradation of dispersed crude oil in the sea", *Chemosphere,* 90:521-526, 2013.

Settles, G.S., *Schieren and Shadowgraph Techniques: Visualizing Phenomena in Transparent Media*, Springer Verlag, 2001.

Slangen, P., L. Aprin, M. Fuhrer, S. Le Floch, and G. Dusserre, "Methyl Ethyl Ketone Spills in Water: Visualisation of the Releases by Optical Schlieren Technique", *Proceedings of 33th AMOP Technical Seminar on Environmental Contamination and Response*, Environment Canada, Ottawa, Ontario, Canada, 7-9 June, 2010.

Yapa, P.D. and F. Chen, "Behavior of Oil and Gas from Deepwater Blowout", *Journal of Hydraulic Engineering*, 130:540-553, 2004.